Published in final edited form as:
Exp Neurol. 2010 April ; 222(2): 267–276. doi:10.1016/j.expneurol.2010.01.004.

Transient elevation of adult hippocampal neurogenesis after dopamine depletion

June-Hee Park and **Grigori Enikolopov***
Cold Spring Harbor Laboratory Cold Spring Harbor, NY 11724

Abstract

Degeneration of the midbrain dopaminergic neurons during Parkinson's disease (PD) may affect remote regions of the brain that are innervated by the projections of these neurons. The dentate gyrus (DG), a site of continuous production of new neurons in the adult hippocampus, receives dopaminergic inputs from the neurons of the substantia nigra (SN). Thus, depletion of the SN neurons during disease or in experimental settings may directly affect adult hippocampal neurogenesis. We show that experimental ablation of dopaminergic neurons in the 1-methyl-4-phenyl-1,2,3,6-tetrahydopyridine (MPTP) mouse model of PD results in a transient increase in cell division in the subgranular zone (SGZ) of the DG. This increase is evident for the amplifying neural progenitors and for their postmitotic progeny; our results also indicate that MPTP treatment affects division of the normally quiescent stem cells in the SGZ. We also show that L-DOPA, used in the clinical treatment of PD, while attenuating the MPTP-induced death of dopaminergic neurons, does not alter the effect of MPTP on cell division in the DG. Our results suggest that a decrease in dopaminergic signaling in the hippocampus leads to a transient activation of stem and progenitor cells in the DG.

Keywords

Parkinson's disease; adult neurogenesis; dentate gyrus; stem cells; MPTP

INTRODUCTION

New neurons are continuously generated in the adult mammalian brain (Gage, et al., 2008, Lledo, et al., 2006, Ming and Song, 2005, Zhao, et al., 2008). Persistent neurogenesis is normally restricted to the subventricular zone (SVZ) of the lateral wall of the lateral ventricles, and the dentate gyrus (DG) of the hippocampus. New neurons are produced from neural stem and progenitor cells after a series of division, elimination, differentiation, and maturation events. Each step of this differentiation cascade can be affected by a variety of intrinsic and extrinsic factors, among them neurotransmitters such as dopamine (Lledo, et al., 2006, Zhao, et al., 2008). Furthermore, adult neurogenesis is strongly affected by aging and disease. Parkinson's disease (PD), in particular, may have a profound effect on adult neurogenesis, with results from both *in vitro* and *in vivo* settings indicating that dopamine is a potent regulator of proliferation of neural progenitors (Baker, et al., 2004, Borta and

*Corresponding author: Grigori Enikolopov enik@cshl.edu (516) 367-8316.

Hoglinger, 2007, Dawirs, et al., 1998, Freundlieb, et al., 2006, Hoglinger, et al., 2004, Kippin, et al., 2005, O'Keeffe, et al., 2009, Peng, et al., 2008, Yang, et al., 2008). The neurogenic regions of the adult brain are innervated by dopaminergic projections from the substantia nigra (SN) and ventral tegmental area (VTA) (Gasbarri, et al., 1997, Gasbarri, et al., 1994, Scatton, et al., 1980, Swanson, 1982, Verney, et al., 1985); therefore, the reduction of the dopamine levels caused by the disease may directly affect the production of new neurons in the SVZ and DG. Given the possible link between production of new neurons and mood disorders and olfaction (Sahay, et al., 2007, Warner-Schmidt and Duman, 2006, Zhao, et al., 2008), it is conceivable that inadequate neurogenesis in the SVZ and DG may underlie depression and impairment of olfaction which often accompany PD.

The specific cell populations and the stages of the neuronal differentiation cascade affected by dopamine are not known. Moreover, the effect of dopamine on neurogenesis may be complex and this neurotransmitter has been described both as a positive and a negative regulator of neurogenesis and neural stem/progenitor cell proliferation. Dopamine receptor antagonists and dopamine depletion have been reported to reduce cell proliferation in the SVZ and DG of rodents and primates (Baker, et al., 2004, Borta and Hoglinger, 2007, Freundlieb, et al., 2006, Hoglinger, et al., 2004, O'Keeffe, et al., 2009, Yang, et al., 2008); however, exposure to dopamine antagonists and ablation of dopaminergic neurons have also been reported to induce neural stem/progenitor cells division (Dawirs, et al., 1998, Kippin, et al., 2005, Peng, et al., 2008). The outcome of the changes in the dopamine levels may reflect a differential response of dopamine receptors and transporters to the variations in the neurotransmitter's levels, activation of compensatory mechanisms, specifics of the animal models, as well as the stage of the disease progression.

We here investigated the effect of dopamine depletion on hippocampal neurogenesis in the 1-methyl-4-phenyl-1,2,3,6-tetrahydopyridine (MPTP) animal model of PD (Bove, et al., 2005, Jackson-Lewis and Przedborski, 2007). Our results indicate that ablation of dopaminergic neurons leads to a transient elevation of hippocampal neurogenesis and that the destruction of dopaminergic neurons in the SN may be the main cause of this elevation. They further indicate that levodopa (L-DOPA) modulates the effect of the ablation and that both the quiescent and the amplifying populations of neural progenitors in the DG may be the main targets of the changed dopamine levels. These results suggest a stage-dependent effect of dopamine depletion on DG neurogenesis.

MATERIALS AND METHODS

Animals

Adult male C57BL/6 mice were used for all experiments (11–15 weeks old at the onset of experiment; purchased from Taconic Farms, Inc., NY). Animals were housed in a standard light- and temperature-controlled environment (12 hr light/dark cycle; light on at 7:00 a.m.; t=21±2°) and access to food and water *ad libitum*. All procedures were approved by Animal Care and Use Committees of Cold Spring Harbor Laboratory, and the protocols are in accordance with Guidelines for the Use and Treatment of Animals by National Institutes of Health.

MPTP, L-DOPA, and BrdU treatment

The mice received a series of four intraperitoneal (i.p.) injections of 20 mg/kg MPTP hydrochloride, dissolved in saline (2 mg MPTP/ml), at 2 hr intervals for a total of 80 mg/kg. MPTP handling and safety followed established guidelines (Jackson-Lewis and Przedborski, 2007). Animals in the control groups received an equivalent volume of saline (10 μl/g body weight). Mice received a single injection of 5-bromo-2'-deoxyuridine (BrdU, 150 mg/kg) to

label proliferating cells 24 hr before euthanasia at 4 days, 7 days or 14 days (day 1 being the date of MPTP injection). In the experiments with L-DOPA we used two schemes of treatment: in one set of experiments, mice were daily treated with L-DOPA (methyl-L-DOPA hydrochloride, 15 mg/kg, i.p.) 1 day after the last MPTP treatment for 12 days and sacrificed at day 14; in the second set of experiments, mice received daily the same amount of L-DOPA for 14 days, starting at 15 days after the last MPTP treatment. Twenty minutes before the L-DOPA treatment, the mice received benserazide hydrochloride (BZ, 12.5 mg/kg, i.p.), a peripheral DOPA decarboxylase inhibitor which increases the production of dopamine from L-DOPA in the brain. Animals in the control groups received an equivalent volume of saline (10 μl/g body weight) without BZ and L-DOPA. Mice were injected with BrdU (150 mg/kg) to label proliferating cells 24 hr before euthanasia at 4 days or 30 days. All reagents were purchased from Sigma. Number of animals per experimental group is indicated in the legends to the figures and results for individual animals are shown as black dots on the histograms.

Tissue preparation

Animals were deeply anesthetized with an overdose of chloral hydrate (150 mg/kg) and transcardially perfused with 30 ml of PBS, followed by 30 ml of 4% paraformaldehyde (PFA) in PBS, pH 7.4. The harvested brains were post-fixed with 4% PFA overnight and stored in PBS with 0.1% sodium azide. The brain was embedded in 2% agarose and 50 mm thick sagittal sections were collected from lateral to midline using Vibratome 1500. Every sixth section was processed for immunohistochemistry.

Immunohistochemistry

Immunohistochemical analysis was performed as described previously (Encinas and Enikolopov, 2008). Briefly, the brain sections were treated with 2N HCl at 37° for 1 hr (for the subsequent detection of BrdU) and neutralized with 0.1 M borate, pH 8.5 for 10 min twice. The sections were then washed three times with washing solution (PBS with 0.2% TritonX-100) and incubated in the blocking solution (PBS containing 3% normal goat serum and 0.2% TritonX-100) for 30 min at room temperature. After rinsing, the sections were incubated overnight at 4° with primary antibodies diluted in the blocking solution as follows: rat anti-BrdU (1:300, Accurate Chemical Inc., OBT-0030), rabbit anti-prospero-related homeobox-1 (Prox-1, 1:2,000, Chemicon Inc., AB-5475), mouse anti-proliferating cell nuclear antigen (PCNA, 1:200, Chemicon Inc., MAB-424), mouse anti- polysialylated neural cell adhesion molecule (PSA-NCAM, 1:400, Chemicon Inc., MAB-5324), mouse anti-tyrosine hydroxylase (TH) (1:4,000, Sigma, T-2928), rabbit anti-brain lipid-binding protein (BLBP, 1:1,000, Chemicon Inc., AB-9558), rabbit anti-Iba-1 (1:2,000, Wako Chemicals, 019-19741). The sections were washed with the washing solution and secondary antibodies (1:400 dilution, Molecular Probes, Alexa Fluor [AF] 488, AF568, or AF633), appropriate for the host of the primary antibody, were applied in the blocking solution. Two hours after the incubation, the sections were washed and mounted with fluorescent mounting medium (DakoCytomation). For counting TH and PSA-NCAM immunoreactive (IR) cells, the sections were processed using a Vectastain ABC-kit (Vector Laboratories). IR signals were developed using a coupled reaction of horse radish peroxidase and glucose oxidase. Briefly, immunolabeled cells were visualized after Vectastain ABC reaction which is based on glucose oxidase reaction (1.3 mg glucose oxidase with 0.1 g β-D-glucose, 0.02 g ammonium chloride, and 1.21 g ammonium nickel sulfate in 50 ml of 0.2 M acetate, pH 4.0) in which β-D-glucose is oxidized at a constant rate to D-gluconolactone and hydrogen peroxide, with chromogen 3,3'-diaminobenzidine (DAB, 10 mg) to visualize the product. After terminating the reaction with distilled water, the sections were mounted on slides, dehydrated through a graded series of ethanol incubations, cleared in xylene, and

coverslipped with DPX mounting medium (VWR Inc.). All reagents, if not mentioned specifically, were purchased from Sigma.

Confocal microscopy and quantification

We obtained fluorescent images by using confocal microscope (Carl Zeiss-LSM510) equipped with a 488 nm and 568 nm argon laser and a 633 nm HeNe laser. The configuration and the detection channels were set according to the manufacture specification, including the main and secondary dichroic beam splitter, band pass filter (BP) and high pass filter (LP); BP 505–530 was assigned for the detection of fluorescent secondary antibody AF488, BP 585–615 for the AF568, and LP 650 for the AF633 under a multitrack mode. We first scanned the DG under a 10× objective lenses and the region containing immunoreactive signals was additionally analyzed under magnification using a 63× objective lenses. In order to count $BrdU^+BLBP^+$ double-labeled cells, twenty optical z serial sections were collected at 2.5 μm intervals from the lower bottom to the top covering the entire 50 μm thick section. We used a maximized scan condition (frame size, X 256 and Y 256; scan speed, 9; scan average, unidirection). We counted manually immunolabeled cells after making three-dimensional images from the optical z sections using Zeiss LSM image browser. We obtained representative images using a pinhole setting of 130 μm for all three channels, with an optical slice less than 1.0 μm. To count the TH and PSA-NCAM IR cells, DAB-mediated immunostained sections were imaged using an upright microscope (Carl Zeiss) connected to a CCD camera. Using the Cell Counter program of the NIH ImageJ software, we counted TH-IR cells of the captured microphotographs; the medial lemniscus (*ml*) and the medial terminal nucleus of the accessory optic tract (*MT*) were used as topographic markers for the SN and the VTA. We quantified the TH IR cells of the substantia nigra pars compacta (SNpc) (lateral 0.24 mm–1.80 mm from the midline) and those of the VTA (lateral 0.24 mm–0.90 mm from the midline) (Franklin and Paxinos, 1997). The counting was blind, with the information on each group and animals sealed and only revealed after counting. We obtained a single tile image of the brain sections immunolabeled for TH using Mosaic module in Axiovision Rel. (Carl Zeiss) from as series of images with 20% overlap.

Statistical analysis

Data are presented as the mean ± SEM. Comparisons between groups were performed using parametric and nonparametric statistical methods as specified in the text and linear regression analysis was performed with GraphPad Prism4 (GraphPad Software, Inc.). Histograms were charted using SigmaPlot 8.0.

RESULTS

Neurotoxin MPTP destroys dopaminergic neurons and their fibers

To examine the effect of dopamine innervation on adult hippocampal neurogenesis, we selectively ablated dopaminergic neurons by exposing mice to the neurotoxin MPTP (4 injections of 20 mg/kg MPTP with 2 hr intervals, with the control group receiving saline injections) (Bove, et al., 2005, Jackson-Lewis and Przedborski, 2007). To characterize the effect of MPTP on dopaminergic neurons and on hippocampal neurogenesis, we analyzed the animals 4, 7, 14, and 30 days after the MPTP treatment, injecting thymidine analog 5-bromo-2-deoxyuridine (BrdU) 24 hrs before the analysis (n=5 for each time point) (Fig. 1A). We detected dopaminergic neurons by immunolabeling for tyrosine hydroxylase (TH) and dividing cells by immunolabeling for BrdU.

Exposure to MPTP induced significant loss of dopaminergic neurons in the SNpc and the VTA and of their axons in the striatum and nucleus accumbens (NAc) (Fig. 1B, C). The loss

of TH-positive neurons and fibers was evident 4 and 7 days after MPTP treatment and was highly pronounced 14 days after the treatment. The number of TH-positive cells in the SNpc and the VTA decreased (as compared to the saline control) by 30.2% and 28.8%, respectively, 7 days after the treatment; 14 days after the treatment the numbers decreased by 26.6% and 30.7%, respectively. Even at the stage when the number of TH-positive cells in the SN had not shown a statistically significant decrease (4 days after the MPTP treatment), there was a large number of activated Iba1-positive microglial cells in the region, closely overlapping the zones of the degenerating TH neurons in the SNpc and substantia nigra pars reticulata (SNpr) (Fig. 1D). Some of the Iba1-positive activated microglial cells were dividing, as evident by BrdU labeling; their fraction was particularly high in SNpc (Fig. 1E). Notably, we did not observe BrdU incorporation into the TH-positive neurons of the SNpc or SNpr, with or without the MPTP treatment. Together, these results demonstrate that MPTP selectively destroyed dopaminergic neurons in the SN and VTA and their fibers in the striatum and NAc and that this process was accompanied by the activation and division of microglial cells in the SN.

Exposure to MPTP increases cell division in the DG

We next examined the MPTP-induced changes in cell division in the DG. 4 and 7 days after the treatment the number of BrdU-labeled cells in the neurogenic zones of the DG of MPTP-treated animals did not change compared to the saline-treated controls. However, 14 days after the treatment the number of labeled cells in the DG of MPTP-treated animals was significantly higher (208%) than in the saline-treated controls; 30 days after the treatment the number of labeled cells in both groups did not differ (Fig. 1F). As an alternative to DNA labeling with BrdU, we counted the number of cells immunoreactive for proliferating cell nuclear antigen (PCNA), an endogenous marker of cell division (Fig. 1G). The results (although numerically slightly higher than for BrdU labeling, as typical of the PCNA-labeled cell populations (Yu, et al., 1992), confirmed that the number of dividing cells in the DG significantly increased (168%) 14 days after MPTP treatment and then decreased to control levels. The bulk of the dividing cells in the DG were in the subgranular zone (SGZ) of the DG, where neural stem and progenitor cells reside in the adult hippocampus; in the MPTP-treated animals some BrdU-labeled cells, possibly corresponding to microglia, were also observed in the molecular layer of the DG (Fig. 1H). To determine whether dividing cells in the SGZ correspond to neural progenitors, we probed the DG sections of mice 14 days after the MPTP treatment with an antibody to brain lipid-binding protein (BLBP), a marker of early stem and progenitor cells (Enikolopov and Overstreet-Wadiche, 2008,Kempermann, et al., 2004). The majority of BrdU-labeled cells in the SGZ of control and MPTP-labeled animals were immunoreactive for BLBP (Fig. 1H). Together, the results of BrdU-, PCNA-, and BLBP labeling confirm that exposure to MPTP transiently induces division of neuronal progenitors in the SGZ.

L-DOPA counteracts the effects of MPTP on cell death but not on cell division in the DG

A precursor to dopamine, L-DOPA, is used clinically to ameliorate motor impairments during PD (Fahn, et al., 2004, Olanow, et al., 2009). We asked whether L-DOPA can affect the MPTP-induced loss of dopaminergic neurons in the SN and VTA and the increase in cell division in the DG. Animal cohorts receiving MPTP or saline have also received injections of L-DOPA (15 mg/kg, administered together with 12.5 mg/kg of benserazide hydrochloride, a peripheral DOPA decarboxylase inhibitor which increases the levels of L-DOPA-derived dopamine in the brain) for 12 days, starting either 1 or 15 days after the last injection of MPTP (Fig. 2A).

As in the previous series of experiment, MPTP exposure destroyed a large fraction of the TH-positive neurons in the SNpc and VTA (38.9% and 41.5%, respectively) and the TH-

positive fibers in the striatum and NAc (Figs. 2B, C). L-DOPA alone did not induce noticeable changes in the distribution or the number of the TH-positive neurons. However, when started immediately after MPTP treatment, L-DOPA administration significantly inhibited the MPTP-induced loss of neurons in the SNpc and noticeably suppressed the loss of TH-positive fibers in the striatum and NAc (Fig. 2B).

We next examined the effect of L-DOPA administration on cell division in the DG. As in the previous series of experiments, MPTP increased the number of dividing (BrdU-labeled) cells in the SGZ 14 days after the treatment (Fig. 2D, E). L-DOPA administration alone did not affect progenitor cell division in the DG and its administration immediately following MPTP treatment did not alter the effect of MPTP (Fig. 2D, Ea. When L-DOPA was administered starting at 15 days after the MPTP treatment, it did not affect the number of BrdU-labeled cells neither when administered alone nor in combination with MPTP (Fig. 2Eb).

Interestingly, the variance of the values of the BrdU-labeled cells' number was significantly higher for the MPTP-exposed groups (with and without L-DOPA) than for the saline- or L-DOPA-treated groups ($p<0.005$ in the Bartlett's test) (Fig. 2E; a similar trend is seen in Fig. 1F). This suggests that the response to the MPTP treatment is highly variable between individual animals and may reflect the extent of damage to the populations of dopaminergic neurons. We therefore analyzed the relationship between the BrdU incorporation and the number of TH-positive cells in the SNpc and the VTA in individual animals. Linear regression analysis indicates that the number of BrdU-labeled cells in the DG was inversely related to the number of TH-positive cells in the SNpc for the MPTP+L-DOPA-treated animals ($r^2=0.4447$, $p=0.0498$) but not in the SNpc of other groups or in the VTA of all 4 groups (Fig. 2F). Together, the results of these experiments suggest that while L-DOPA suppresses the dopaminergic neuron-directed toxicity of MPTP, it does not noticeably alter the effect of MPTP on cell division in the DG.

MPTP stimulates division of neural stem cells in the DG

We next sought to determine the class of progenitor cell in the DG whose proliferation was increased by MPTP. There are several population of neural progenitors in the DG, including a subclass of highly quiescent cells (described as Type1 cells, radial glia-like progenitors, and quiescent neural progenitors, QNPs) corresponds to stem cells of the DG; a subclass of actively dividing cells corresponds to the transit-amplifying progeny of stem cells (described as Type 2a cells, intermediate neural progenitors, and amplifying neural progenitors, ANPs); and a subclass of postmitotic progenitors which gradually mature into differentiated granule neurons (described as Type 3 cells, D-type cells, and neuroblasts, NB) (Encinas, et al., 2006, Enikolopov and Overstreet-Wadiche, 2008, Filippov, et al., 2003, Kempermann, et al., 2004, Mignone, et al., 2004, Seri, et al., 2004, Steiner, et al., 2006). QNPs, ANPs, and NBs can be identified by a set of expressed protein markers or the expression of reporter transgenes (Encinas, et al., 2006, Enikolopov and Overstreet-Wadiche, 2008, Kempermann, et al., 2004). In particular, antibody to BLBP identifies QNPs and a subset of ANPs (during a short period after their birth from the QNPs), whereas antibody to PSA-NCAM reveals NBs. Treatment with MPTP and MPTP+L-DOPA (but not with L-DOPA alone) increased the number of BrdU-positive (Figs. 1F, 2E, and 3A) and BLBP-positive $BrdU^+$ cells in the SGZ (Fig. 3A–D), when analyzed 14 days later. The number of BrdU-positive cells was also increased in the molecular layer; however, these cells did not express BLBP (corresponding, probably, to microglial cells) (Fig. 3B).

Within the dividing cells in the SGZ, the largest fraction (~95%) is represented by ANPs, with a minority of the BrdU-positive population represented by QNPs (~4%) and oligodendrocytes precursor cells (OPCs) (~1%). The number of $BrdU^+BLBP^+$ QNPs

increased in response to the MPTP and MPTP+L-DOPA treatments and was not affected by the treatment with L-DOPA alone (Fig. 3C). The number of $BrdU^+$ ANPs (including those that express BLBP and ceased to express BLBP) was also significantly increased in response to MPTP and MPTP+L-DOPA but not L-DOPA alone (Fig. 3D). The fraction of the QNP and ANP cells within the population of labeled cells in the SGZ did not vary significantly in response to the treatment (Fig. 3E). Since the variance of the values' distribution was again larger for the MPTP-exposed groups, we analyzed the representation of subclasses of labeled cells among all labeled cells in the SGZ and the relation between those subclasses and the TH-expressing cells in the SNpc and the VTA. We found that the number of $BrdU^+BLBP^+$ QNPs was significantly correlated (r^2=0.4615, p=0.0442) with the number of all $BrdU^+$ cells in the MPTP+L-DOPA group, but not in other groups (Fig. 3F); the number of BrdU-positive ANP cells was correlated with the total number of $BrdU^+$ cells for all 4 groups of animals, as expected (since they represent the bulk of the BrdU-positive population in the SGZ) (Fig. 3G). When the relation between the BrdU-labeled cells in the SGZ and the TH-labeled cells in the midbrain was analyzed, we found a significant inverse correlation between the number of BrdU-labeled ANPs and the number of the TH-positive neurons in the SNpc in the MPTP+L-DOPA group (r^2=0.4625, p=0.0438) (Fig. 3H), but not in other groups; we also did not see any correlation for any of the groups when compared to the TH-neurons in the VTA.

We next analyzed the changes in the PSA-NCAM-expressing postmitotic progenitor cells (NBs) in the DG of the treated animals. The number of PSA-NCAM-labeled cells was significantly increased in the MPTP+L-DOPA group as compared to the L-DOPA-treated group (Fig. 4A, B). Since postmitotic progenitors start to migrate away from the SGZ, we analyzed the distribution of the PSA-NCAM-positive cells within the subregions of the DG — the SGZ, the inner granular zone (IGZ; we combined the numbers in the SGZ and the IGZ because of uncertainty in ascribing individual PSA-NCAM-positive cells to each group), the middle granular zone (MGZ), and the outer granular zone (OGZ). Although the bulk of PSA-NCAM immunoreactive cells remained in the SGZ and IGZ, MPTP and L-DOPA treatments introduced significant changes in the number of PSA-NCAM cells in all three layers; furthermore, the fraction of cells moving to the MGZ and OGZ was also increased in the MPTP− and MPTP+L-DOPA-treated animals. Together, our results suggest that exposure to MPTP and L-DOPA affects dividing progenitors and their postmitotic progeny in the neurogenesis cascade in the DG.

DISCUSSION

Dopaminergic neurons of the SN and VTA send numerous projections to distant regions of the brain (Gasbarri, et al., 1997, Gasbarri, et al., 1994, Scatton, et al., 1980, Swanson, 1982, Verney, et al., 1985); thus, degeneration of the SN dopaminergic neurons, a hallmark of Parkinson's disease, may have profound consequences for these remote regions. In particular, major dopaminergic projections from the midbrain are found in the hippocampal formation and the DG, the site of persistent adult neurogenesis; importantly, PD patients show a significant decrease in dopamine levels in the hippocampus (Lang and Obeso, 2004, Schapira, et al., 2006). The mechanisms of dopamine action on the division of neural precursors is insufficiently understood, with results from different i*n vivo* and *in vitro* experimental systems reporting opposite effects of dopamine addition or depletion. For instance, destruction of dopaminergic neurons decreases neurogenesis in the SVZ and DG in rodents and primates *in vivo* (Baker, et al., 2004, Freundlieb, et al., 2006, Hoglinger, et al., 2004); however, in a similar experimental setting and in *in vitro* experiments with dopamine receptor antagonists, suppression of the dopamine signaling has been reported to have an opposite effect, suggesting a role for dopamine as a negative regulator of division of neural progenitors (Dawirs, et al., 1998, Kippin, et al., 2005, Peng, et al., 2008). These conflicting

results may reflect a complex and multifunctional nature of the dopamine signaling in dividing cells; furthermore, they may reflect some compensatory mechanisms that are activated to help the nervous system cope with the disease.

We here show that treatment with the dopaminergic neuron-specific toxin MPTP results in a transient elevation of cell division in the DG. This elevation is evident 14 days after the treatment; after 30 days the number of dividing cells in the DG returns to the control levels. While we do not know the mechanism of this transient elevation, it is conceivable that the temporary increase in stem and progenitor division reflects a combination of immediate and compensatory changes in the vicinity of neurogenic zones or in neural progenitors themselves, elicited in response to the changes in dopamine signaling. Our results highlight a complex dependence of neurogenesis on dopamine stimulation and may help reconcile the reports in which seemingly opposite directions of change in the DG in the MPTP model have been observed (Hoglinger, et al., 2004, Peng, et al., 2008).

Our results indicate that transient MPTP-induced increase in cell division in the DG may reflect activation of the DG stem cells, normally a highly quiescent population of neural progenitors. Interestingly, activation of stem cells has been also reported for other models of neurodegeneration and may reflect a general compensatory mechanism that attempts to restore the neuronal loss by activating division of stem cells (Curtis, et al., 2005, Gao, et al., 2009, Jin, et al., 2004, Kunze, et al., 2006, Parent, et al., 2006, Yu, et al., 2008); note, however, we did not find evidence for neurogenesis in the SN, with or without the MPTP treatment. Post mortem studies of the PD brains show a decreased number of radial glia cells (analogous to the QNP stem cells in our model) and a reduced number of dividing cells in the hippocampus (Hoglinger, et al., 2004), perhaps reflecting the effect of chronic progressive neurodegeneration that cannot be compensated by the proliferative resources of hippocampal stem cells.

Our results indicate that L-DOPA has neuroprotective effect on dopaminergic neurons when applied immediately after MPTP. However, while attenuating the loss of TH-neurons in the SNpc, L-DOPA does not sufficiently alter the effects of MPTP on hippocampal neurogenesis. This may reflect the possibility that L-DOPA-induced suppression of neuronal death is insufficient to fully compensate for the effect of neuronal loss on hippocampal neurogenesis (e.g., if neurogenesis is exquisitely sensitive to the levels of dopamine), or the possibility that neurogenesis reacts to more subtle effects of MPTP (e.g., perturbations of dopamine receptor signaling).

Adult hippocampal neurogenesis is associated with learning and memory as well as stress, depression, and response to antidepressant therapies (Sahay, et al., 2007, Warner-Schmidt and Duman, 2006, Zhao, et al., 2008). There is high comorbidity between PD and depression, with over 50% of PD patients reported to experience symptoms of depression; moreover, depression may precede the manifestation of the motor deficits in PD patients (Chaudhuri and Schapira, 2009, Mentis and Delalot, 2005, Vajda and Solinas, 2005). Therefore, it is conceivable that changes in adult neurogenesis may be related to the etiology of depression in PD and may affect the response of the PD patients to antidepressants. Further investigations of the neural stem cells' response to altered levels of dopamine may help elucidate the link between the death of dopaminergic neurons and the cognitive sequelae of PD.

Acknowledgments

We are grateful to Serge Przedborski (Columbia University) for advice. We thank our lab members Juan Manuel Encinas, Tatyana Michurina and Natalia Peunova for help and advice, Stephen Hearn (CSHL) for help with microscopy, and Lisa Bianco and Jodi Coblentz (CSHL) for their help with the animal studies. This work was

supported by The Hartman Foundation for Parkinson's Research, National Institute of Mental Health, National Alliance for Research on Schizophrenia and Depression (NARSAD), Hope for Depression Foundation, Cody Center for Autism and Developmental Disabilities, The Robertson Foundation, The Charles Leach II Foundation, and The Ira Hazan Foundation to G.E. J.-H. P. was supported by the Young Investigator Award from NARSAD and by fellowship of the Korea Research Foundation (KRF-2005-214-C00224).

REFERENCES

1. Baker SA, Baker KA, Hagg T. Dopaminergic nigrostriatal projections regulate neural precursor proliferation in the adult mouse subventricular zone. Eur J Neurosci 2004;20:575–579. [PubMed: 15233767]
2. Borta A, Hoglinger GU. Dopamine and adult neurogenesis. J Neurochem 2007;100:587–595. [PubMed: 17101030]
3. Bove J, Prou D, Perier C, Przedborski S. Toxin-induced models of Parkinson's disease. NeuroRx 2005;2:484–494. [PubMed: 16389312]
4. Chaudhuri KR, Schapira AHV. Non-motor symptoms of Parkinson's disease: dopaminergic pathophysiology and treatment. Lancet Neurology, The 2009;8:464–474.
5. Curtis MA, Penney EB, Pearson J, Dragunow M, Connor B, Faull RL. The distribution of progenitor cells in the subependymal layer of the lateral ventricle in the normal and Huntington's disease human brain. Neuroscience 2005;132:777–788. [PubMed: 15837138]
6. Dawirs RR, Hildebrandt K, Teuchert-Noodt G. Adult treatment with haloperidol increases dentate granule cell proliferation in the gerbil hippocampus. J Neural Transm 1998;105:317–327. [PubMed: 9660110]
7. Encinas JM, Enikolopov G. Identifying and Quantitating Neural Stem and Progenitor Cells in the Adult Brain. Methods Cell Biol 2008;85C:243–272. [PubMed: 18155466]
8. Encinas JM, Vaahtokari A, Enikolopov G. Fluoxetine targets early progenitor cells in the adult brain. Proc Natl Acad Sci U S A 2006;103:8233–8238. [PubMed: 16702546]
9. Enikolopov, G.; Overstreet-Wadiche, L. Transgenic reporter lines for studying adult neurogenesis. In: Gage, F.; K., G.; Song, H., editors. Adult Neurogenesis. CSHL Press; 2008.
10. Fahn S, Oakes D, Shoulson I, Kieburtz K, Rudolph A, Lang A, Olanow CW, Tanner C, Marek K. Levodopa and the progression of Parkinson's disease. N Engl J Med 2004;351:2498–2508. [PubMed: 15590952]
11. Filippov V, Kronenberg G, Pivneva T, Reuter K, Steiner B, Wang LP, Yamaguchi M, Kettenmann H, Kempermann G. Subpopulation of nestin-expressing progenitor cells in the adult murine hippocampus shows electrophysiological and morphological characteristics of astrocytes. Mol Cell Neurosci 2003;23:373–382. [PubMed: 12837622]
12. Franklin, KBJ.; Paxinos, G. The mouse brain in stereotaxic coordinates. Academic Press; San Diego: 1997.
13. Freundlieb N, Francois C, Tande D, Oertel WH, Hirsch EC, Hoglinger GU. Dopaminergic substantia nigra neurons project topographically organized to the subventricular zone and stimulate precursor cell proliferation in aged primates. J Neurosci 2006;26:2321–2325. [PubMed: 16495459]
14. Gage, F.; Kempermann, G.; Song, H.; Cold Spring Harbor Laboratory. Adult neurogenesis. Cold Spring Harbor Laboratory Press; Cold Spring Harbor, N.Y.: 2008.
15. Gao X, Enikolopov G, Chen J. Moderate traumatic brain injury promotes proliferation of quiescent neural progenitors in the adult hippocampus. Exp Neurol. 2009
16. Gasbarri A, Sulli A, Packard MG. The dopaminergic mesencephalic projections to the hippocampal formation in the rat. Prog Neuropsychopharmacol Biol Psychiatry 1997;21:1–22. [PubMed: 9075256]
17. Gasbarri A, Verney C, Innocenzi R, Campana E, Pacitti C. Mesolimbic dopaminergic neurons innervating the hippocampal formation in the rat: a combined retrograde tracing and immunohistochemical study. Brain Res 1994;668:71–79. [PubMed: 7704620]
18. Hoglinger GU, Rizk P, Muriel MP, Duyckaerts C, Oertel WH, Caille I, Hirsch EC. Dopamine depletion impairs precursor cell proliferation in Parkinson disease. Nat Neurosci 2004;7:726–735. [PubMed: 15195095]

19. Jackson-Lewis V, Przedborski S. Protocol for the MPTP mouse model of Parkinson's disease. Nat Protoc 2007;2:141–151. [PubMed: 17401348]
20. Jin K, Galvan V, Xie L, Mao XO, Gorostiza OF, Bredesen DE, Greenberg DA. Enhanced neurogenesis in Alzheimer's disease transgenic (PDGF-APPSw,Ind) mice. Proc Natl Acad Sci U S A 2004;101:13363–13367. [PubMed: 15340159]
21. Kempermann G, Jessberger S, Steiner B, Kronenberg G. Milestones of neuronal development in the adult hippocampus. Trends Neurosci 2004;27:447–452. [PubMed: 15271491]
22. Kippin TE, Kapur S, van der Kooy D. Dopamine specifically inhibits forebrain neural stem cell proliferation, suggesting a novel effect of antipsychotic drugs. J Neurosci 2005;25:5815–5823. [PubMed: 15958748]
23. Kunze A, Grass S, Witte OW, Yamaguchi M, Kempermann G, Redecker C. Proliferative response of distinct hippocampal progenitor cell populations after cortical infarcts in the adult brain. Neurobiol Dis 2006;21:324–332. [PubMed: 16137890]
24. Lang AE, Obeso JA. Challenges in Parkinson's disease: restoration of the nigrostriatal dopamine system is not enough. Lancet Neurol 2004;3:309–316. [PubMed: 15099546]
25. Lledo PM, Alonso M, Grubb MS. Adult neurogenesis and functional plasticity in neuronal circuits. Nat Rev Neurosci 2006;7:179–193. [PubMed: 16495940]
26. Mentis MJ, Delalot D. Depression in Parkinson's disease. Adv Neurol 2005;96:26–41. [PubMed: 16383210]
27. Mignone JL, Kukekov V, Chiang AS, Steindler D, Enikolopov G. Neural stem and progenitor cells in nestin-GFP transgenic mice. J Comp Neurol 2004;469:311–324. [PubMed: 14730584]
28. Ming GL, Song H. Adult neurogenesis in the mammalian central nervous system. Annu Rev Neurosci 2005;28:223–250. [PubMed: 16022595]
29. O'Keeffe GC, Tyers P, Aarsland D, Dalley JW, Barker RA, Caldwell MA. Dopamine-induced proliferation of adult neural precursor cells in the mammalian subventricular zone is mediated through EGF. Proc Natl Acad Sci U S A 2009;106:8754–8759. [PubMed: 19433789]
30. Olanow CW, Stern MB, Sethi K. The scientific and clinical basis for the treatment of Parkinson disease (2009). Neurology 2009;72:S1–136. [PubMed: 19470958]
31. Parent JM, Elliott RC, Pleasure SJ, Barbaro NM, Lowenstein DH. Aberrant seizure-induced neurogenesis in experimental temporal lobe epilepsy. Ann Neurol 2006;59:81–91. [PubMed: 16261566]
32. Peng J, Xie L, Jin K, Greenberg DA, Andersen JK. Fibroblast growth factor 2 enhances striatal and nigral neurogenesis in the acute 1-methyl-4-phenyl-1,2,3,6-tetrahydropyridine model of Parkinson's disease. Neuroscience 2008;153:664–670. [PubMed: 18407421]
33. Sahay A, Drew MR, Hen R. Dentate gyrus neurogenesis and depression. Prog Brain Res 2007;163:697–722. [PubMed: 17765746]
34. Scatton B, Simon H, Le Moal M, Bischoff S. Origin of dopaminergic innervation of the rat hippocampal formation. Neurosci Lett 1980;18:125–131. [PubMed: 7052484]
35. Schapira AH, Bezard E, Brotchie J, Calon F, Collingridge GL, Ferger B, Hengerer B, Hirsch E, Jenner P, Le Novere N, Obeso JA, Schwarzschild MA, Spampinato U, Davidai G. Novel pharmacological targets for the treatment of Parkinson's disease. Nat Rev Drug Discov 2006;5:845–854. [PubMed: 17016425]
36. Seri B, Garcia-Verdugo JM, Collado-Morente L, McEwen BS, Alvarez-Buylla A. Cell types, lineage, and architecture of the germinal zone in the adult dentate gyrus. J Comp Neurol 2004;478:359–378. [PubMed: 15384070]
37. Steiner B, Klempin F, Wang L, Kott M, Kettenmann H, Kempermann G. Type-2 cells as link between glial and neuronal lineage in adult hippocampal neurogenesis. Glia 2006;54:805–814. [PubMed: 16958090]
38. Swanson LW. The projections of the ventral tegmental area and adjacent regions: a combined fluorescent retrograde tracer and immunofluorescence study in the rat. Brain Res Bull 1982;9:321–353. [PubMed: 6816390]
39. Vajda FJ, Solinas C. Current approaches to management of depression in Parkinson's Disease. J Clin Neurosci 2005;12:739–743. [PubMed: 16026985]

40. Verney C, Baulac M, Berger B, Alvarez C, Vigny A, Helle KB. Morphological evidence for a dopaminergic terminal field in the hippocampal formation of young and adult rat. Neuroscience 1985;14:1039–1052. [PubMed: 2860616]

41. Warner-Schmidt JL, Duman RS. Hippocampal neurogenesis: opposing effects of stress and antidepressant treatment. Hippocampus 2006;16:239–249. [PubMed: 16425236]

42. Yang P, Arnold SA, Habas A, Hetman M, Hagg T. Ciliary neurotrophic factor mediates dopamine D2 receptor-induced CNS neurogenesis in adult mice. J Neurosci 2008;28:2231–2241. [PubMed: 18305256]

43. Yu CC, Woods AL, Levison DA. The assessment of cellular proliferation by immunohistochemistry: a review of currently available methods and their applications. The Histochemical journal 1992;24:121–131. [PubMed: 1349881]

44. Yu TS, Zhang G, Liebl DJ, Kernie SG. Traumatic brain injury-induced hippocampal neurogenesis requires activation of early nestin-expressing progenitors. J Neurosci 2008;28:12901–12912. [PubMed: 19036984]

45. Zhao C, Deng W, Gage FH. Mechanisms and functional implications of adult neurogenesis. Cell 2008;132:645–660. [PubMed: 18295581]

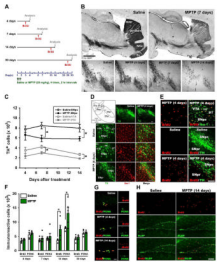

Figure 1. Treatment with MPTP induces transient increase in dividing cells in the DG

(A) Scheme of the experiment. Adult male mice were treated with MPTP or saline on day 1 and BrdU was injected 24 hr before each euthanasia point on the 4th, 7th, 14th, and 30th day (n=5 for each time point).

(B) Single tile images of sagittal brain sections immunostained for tyrosine hydroxylase (TH). MPTP treatment destroys dopaminergic neurons in the midbrain and their axon fibers in the striatum and nucleus accumbens (NAc). Top row - saline- or MPTP-treated animals 7 days after the treatment; bottom row — higher magnification of the midbrain region 4, 7, or 14 days after the MPTP treatment or 14 days after saline treatment (control). Note the gradual disappearance of TH-stained dopaminergic neurons in the VTA and SN and loss of TH-positive fibers in the striatum and NAc.

(C) Quantification of TH-immunoreactive (IR) cells in the SNpc and VTA. MPTP treatment results in a significant loss of TH IR neurons in the SNpc and VTA on the 7th and 14th day after the treatment compared to saline-treated controls (n=5 for each time point). Error bars show s.e.m. *$p \leq 0.05$ in Student's unpaired *t*-test.

(D) Fluorescent Immunostaining for TH and Iba-1, a marker of microglia, 4 days after the MPTP or saline treatment. MPTP induces loss of TH-positive dopaminergic neurons in SN and VTA (top row). Hypertrophic Iba-1-stained microglia is seen near the VTA (third row) and the SNpc (bottom row).

(E) Fluorescent immunostaining for BrdU, Iba-1, and TH 4 days after the MPTP or saline treatment in the SNpc, middle, and around the VTA, bottom. Most of the BrdU-labeled newborn cells in the SNpc and around the VTA are co-labeled with Iba-1.

(F) Quantification of BrdU- and PCNA-IR cells in the DG 4, 7, 14, and 30 days after the MPTP treatment, with BrdU injected 24 hrs before the analysis. The results for individual animals are shown as black dots; error bas show s.e.m. *$p \leq 0.05$ in Student's unpaired *t*-test.

(G) Fluorescent immunostaining for BrdU and PCNA in the DG 4 and 14 days after treatment with MPTP or saline.

(H) Fluorescent immunostaining for BrdU and BLBP in the DG 14 days after treatment with MPTP or saline. The majority of newborn cells are in the SGZ, close to radial-glia like BLBP-positive QNP stem cells, below the granular cells layer. Some labeled cells can be seen in the hilus and molecular layer of the MPTP-treated animal brain.

Abbreviations; cp, cerebral peduncle; Hip, hippocampus; LV, lateral ventricle; ml, medial lemniscus; MT, medial terminal nucleus of the accessory optic tract; SGZ, subgranular zone; SVZ, subventricular zone; SNpc, substantia nigra pars compacta; SNpr, substantia nigra pars reticulata; Tu, olfactory tubercle; VTA, ventral tegmental area; NAc; nucleus accumbens.

Scale bars: 1 mm in B; 100 μm (top row) and 10 μm (middle and bottom rows) in D; 100 μm in E; 10 μm in G; 100 μm in H.

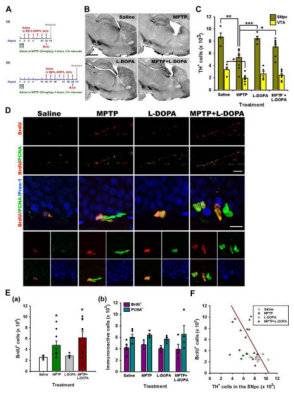

Figure 2. L-DOPA effects on cell death in the midbrain and cell division in the DG

(A) Scheme of the experiment. Adult male mice were treated with MPTP or saline on day 1 and L-DOPA and BZ or saline (control) were injected daily for 12 days, starting 1 or 14 days after the last MPTP injection. BrdU was injected 24 hr before euthanasia.

(B) Single tile images of sagittal brain sections immunostained for tyrosine hydroxylase (TH). The loss of dopaminergic neurons and fibers is evident in the midbrain, striatum, and NAc and of their axon fibers in the striatum and nucleus accumbens (NAc). Top row - saline- or MPTP-treated animals; bottom row – L-DOPA or MPTP+L-DOPA 14 days after the treatment. Note that L-DOPA attenuates the MPTP-induced loss of TH-positive dopaminergic neurons in the SNpc and VTA and of their fibers in the striatum and NAc.

(C) Quantification of TH-IR cells in the SNpc and VTA 14 days after the treatment with saline (n=4), MPTP (n=9), L-DOPA (n=5), or MPTP+L-DOPA (n=9). The results for individual animals are shown as black dots; error bas show s.e.m. *$p \leq 0.05$, **$p \leq 0.01$, ***$p \leq 0.001$ compared to the saline-treated group in ANOVA followed by Newman-Keuls post hoc test.

(D) Fluorescent Immunostaining of cells in the DG for BrdU, PCNA and Prox-1. Most of the BrdU- and PCNA-labeled cells are distributed in the SGZ (top two rows, lower magnification), below the Prox-1-labeled granular cells of the DG (middle and bottom rows, showing granular cells and SGZ cells at higher magnification).

(E) Quantification of BrdU-labeled cells in the DG 14 days (a) or 30 days (b) (see scheme in Fig, 3A) after the treatment with saline (n=4 for 14 days and 5 for 30 days), MPTP (n=9 for 14 days and 4 for 30 days), L-DOPA (n=5 for 14 days and 4 for 30 days), or MPTP+L-DOPA (n=9 for 14 days and 4 for 30 days), with BrdU injected 24 hrs before the analysis. The results for individual animals are shown as black dots; error bas show s.e.m. The variance of the values was significantly higher for the MPTP-exposed groups than for the saline- or L-DOPA-treated groups ($p<0.0002$ in the Bartlett's test for the 14 day set), the distribution of values was not Gaussian, and the number of subjects in each groups was different, indicating the use of a non-parametric Kruskal-Wallis test ($p=0.0318$) with the Dunn multiple comparison post hoc test; *$p<0.05$.

(F) The loss of TH-positive dopaminergic neurons in the SNpc and cell division in the DG show a significant linear relationship in the MPTP+L-DOPA group 14 days after the treatment (regression coefficient, $r^2=0.4447$; $p=0.0498$).

Scale bars, 1 mm in B; 100 μm in the top two rows (BrdU/PCNA) in D and 10 μm in the middle row (BrdU/PCNA/Prox-1) in D.

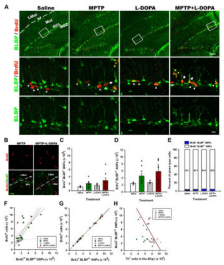

Figure 3. MPTP and L-DOPA affect progenitor cells in the DG

(A) Fluorescent Immunostaining of cells in the DG for BrdU and BLBP. Bracketed areas in the top row are presented at higher magnification in the bottom rows. QNPs are seen as $BrdU^+BLBP^+$ radial glia-like cells with a long basal process (white arrows), ANPs as BrdU +$BLBP^+$ and $BrdU^+BLBP^-$ compact cells with the basal process (white arrowheads), and OPCs as $BrdU^+BLBP^+$ and BrdU+$BLBP^-$ multiprocess cells (yellow arrowheads). Scale bars are 100 μm in the top row and 10 μm in the middle and bottom rows.

(B) MPTP and MPTP+L-DOPA treatments increased cell proliferation in the molecular layer of the DG and stratum lacunosum-molecular of the hippocampus; however, most of the dividing cells were negative for BLBP immunostaining. Scale bar is 10 μm.

(C) Quantification of $BrdU^+BLBP^+$ QNP cells in the DG 14 days after the treatment with saline (n=4), MPTP (n=9), L-DOPA (n=5), or MPTP+L-DOPA (n=9). The results for individual animals are shown as black dots; error bas show s.e.m. The variance of the values was significantly higher for the MPTP-exposed groups than for the saline- or L-DOPA-treated groups ($p<0.0005$ in the Bartlett's test), the distribution of values was not Gaussian, and the number of subjects in each groups was different, indicating the use of a non-parametric Kruskal-Wallis test with the Dunn multiple comparison post hoc test.

(D) Quantification of $BrdU^+BLBP^+$ and $BrdU^+BLBP^-$ ANP cells in the DG 14 days after the treatment with saline (n=4), MPTP (n=9), L-DOPA (n=5), or MPTP+L-DOPA (n=9). The results for individual animals are shown as black dots; error bas show s.e.m. The variance of the values was significantly higher for the MPTP-exposed groups than for the saline- or L-DOPA-treated groups ($p<0.005$ in the Bartlett's test), the distribution of values was not Gaussian, and the number of subjects in each groups was different, indicating the use of a non-parametric Kruskal-Wallis test ($p=0.0307$) with the Dunn multiple comparison post hoc test; $p = 0.052$ for MPTP and 0.058 for MPTP+L-DOPA.

(E) The fraction of BrdU-labeled QNP and ANPs cells among all BrdU-labeled cells in the SGZ. MPTP or L-DOPA treatments did not significantly change the fraction of BrdU-labeled QNP or ANPs cells (*$p>0.05$; Kruskal-Wallis test with the Dunn multiple comparison post hoc test).

(F) The number of $BrdU^+/BLBP^+$ QNP cells shows a significant linear relationship ($r^2=0.4615$ $p=0.0442$) with the number of $BrdU^+$-labeled cells in the MPTP+L-DOPA group.

(G) The number of $BrdU^+$- labeled ANP cells shows a significant linear relationship (saline, $r2=0.9988$, $p=0.0006$; MPTP, $r^2=0.9989$, $p=0.0001$; L-DOPA, $r^2=0.9761$, $p=0.0016$; MPTP +LDOAP, $r^2=0.9973$, $p=0.0001$) with the number of $BrdU^+$-labeled cells in all animal groups.

(H) The loss of TH-positive dopaminergic neurons in the SNpc and cell division in the DG show a significant linear relationship in the MPTP+L-DOPA group ($r^2=0.4625$; $p=0.0438$).

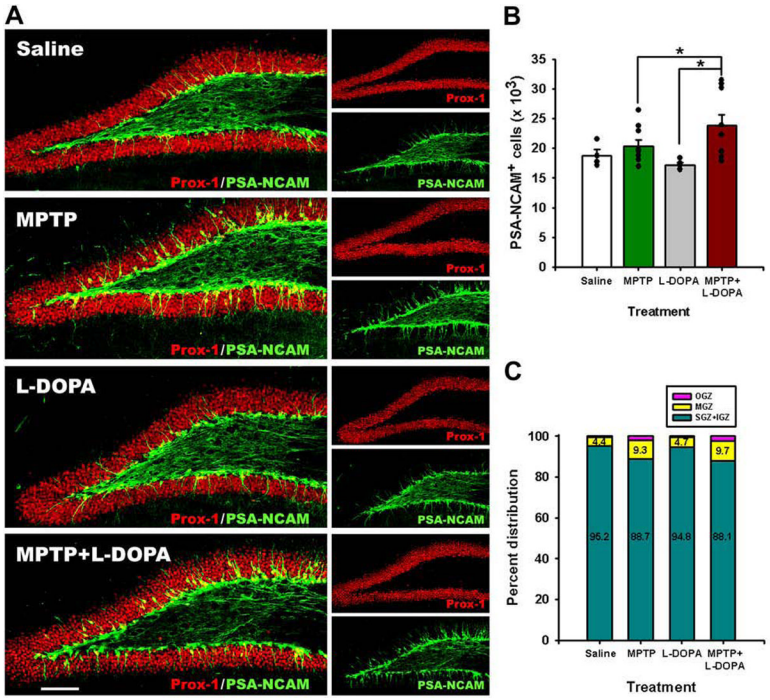

Figure 4. MPTP affects maturation of postmitotic neuronal progenitors in the DG

(A) Fluorescent immunostaining for PSA-NCAM and Prox-1, markers of potsmitioc neuroblasts and young neurons. Note that a fraction of PSA-NCAM- and Prox-1-expressing cells are localized in the middle and outer cell layer of the DG in the MPTP- and MPTP+L-DOPA-treated animals. Scale bar is 100 μm.

(B) Quantification of PSA-NCAM-expressing cells in the DG 14 days after the treatment with saline (n=4), MPTP (n=9), L-DOPA (n=5), or MPTP+L-DOPA (n=9). The results for individual animals are shown as black dots; error bas show s.e.m. MPTP+L-DOPA increased the number of PSA-NCAM-labeled immature neurons in the DG, compared to the MPTP- and L-DOPA treated groups (p=0.0154 in Kruskal-Wallis test with the Dunn multiple comparison post hoc test; *p<0.05).

(C) Distribution of PSA-NCAM expressing cells in different layers of the DG: the subgranular (SGZ), inner (IGZ), middle (MGZ), and outer (OGZ) granular zones of the DG. MPTP and MPTP+L-DOPA treatments increased the fraction of PSA-NCAM-expressing cells in the MGZ and the OGZ of the DG (p=0.0181, 0.0487, and 0.0114 in the Kruskal-Wallis test for the SGZ+IGZ, MGZ, and OGZ, respectively).